Robust Minimum-Time Control with Coarse/Fine Dual-Stage Mechanism

SangJoo Kwon
School of Aerospace and Mechanical Engineering, Hankuk Aviation University, Goyang 412-791, Korea
Joono Cheong*
Department of Control and Instrumentation Engineering, Korea University, Jochiwon 339-770, Korea

A robust minimum-time control (RMTC) strategy is addressed and it is extended to the dual-stage servo design. Rather than conventional switching type sub-optimal controls, it is a reference following control approach where the predetermined minimum-time trajectory (MTT) is tracked by the perturbation compensator based feedback controller. First, the minimum-time trajectory for a mass-damper system is derived. Then, the perturbation compensator to achieve robust tracking performance in spite of model uncertainty and external disturbance is suggested. The RMTC is also applied to the dual-stage positioner which consists of coarse actuator and fine one. To best utilize the actuation redundancy of the dual-stage mechanism, a null-motion controller to actively regulate the relative motion between the two stages is formulated. The performance of RMTC is validated through simulation and experiment.

Key Words : Minimum-Time Control, Perturbation Compensator, Positioning System, Dual-Stage Mechanism, Null-Motion Control

1. Introduction

In many positioning servomechanisms, the minimum-time control is considered as a hot issue to enhance the performance and productivity. Taking some examples, the performance of hard disk drives is directly related to the track seek time of head positioning arm and the pick-and-place speed determines the productivity of a robotic assembly line. Also, the payability of mass production lines in semiconductor or flat panel display manufacturing industry is largely dependant upon how much the overall tact time can be reduced by improving the positioning performance of in-line positioning systems such as panel-mask aligners, probing systems, and visual inspection equipments.

In terms of the optimal control solving procedure, the minimum-time (i.e., time-optimal) control is given as a bang-bang control law : $u(t) = -\mathrm{sgn}(h(x))$ with $h(x)$ the switching function (Athans and Falb, 1966). However, the minimum-time control solution is just a theoretical possibility and it only holds for nominal model with no process noises. In practical situations where the model uncertainty and external disturbance exist, the bang-bang control may occur heavy chattering or limit cycling since exact switching on the switching manifold is actually impossible owing to the discrepancy between the model and the real (Franklin et al., 1990 ; Friedland, 1996).

Hence, a large number of sub-optimal or near minimum-time control strategies to mitigate the

* Corresponding Author,
E-mail : jncheong@korea.ac.kr
TEL : +82-41-860-1449; **FAX** : +82-41-865-1820
Department of Control and Instrumentation Engineering, Korea University, Jochiwon 339-770, Korea. (Manuscript **Received** December 19, 2005; **Revised** August 14, 2006)

chattering phenomena and compromise control performance were announced, e.g., in (Newman and Souccar, 1991 ; Pao and Franklin, 1993) and the references therein. Most of them are basically to avoid severe switching control actions by modifying the switching surface in the vicinity of the target point and introducing a saturation function like instead of the signum function. For example, Franklin et al.(1990) addressed the proximate time-optimal servomechanism (PTOS) and it was extended to 3rd-order systems in (Pao and Franklin, 1993), where the switching control in the tolerance region of target point is replaced by a linear control technique. Newman and Souccar (1991) introduced a boundary layer around the switching function and adopted the sliding mode control technique near the target region for chattering suppression. Also, Kim et al.(1999) proposed a robust time-optimal controller combining the PTOS with an internal-loop compensator.

In all sub-optimal control methods including above examples, the bang-bang control based on the switching function has been retained although approximation schemes are incorporated to meet the robust performance requirement. While, the reliability of the switching function value is entirely dependant upon the exactness of full-state feedback signals and in case that the feedback signals contain large time-delay and measurement noise, the near time-optimality is not maintained anymore. In this regard, the robust minimum-time control (RMTC) as an alternative approach is suggested in this paper. Instead of real-time computing the switching function, we are to determine the minimum-time trajectory (MTT) based on the switching function and design a robust tracking controller to follow it satisfactorily. This approach has the merit of removing switching control fundamentally.

The second issue of this paper is to apply the RMTC to the dual-stage mechanism. Usually, positioning systems are driven by electrical motors or hydraulic servomechanisms, where the servo bandwidth and motion resolution are mainly limited by the stick/slip motion due to the nonlinear friction. On the other hand, the fine actuators which usually make use of piezoelectricity are free of friction and enable much higher bandwidth motion, but their travel ranges are very small. Then, the compound actuation system composed of the coarse/fine dual-stage mechanism can utilize both advantages of the two heterogeneous actuators, where the coarse actuator can provide large power and long travel range while the fine one enables fast and fine motions (Yen et al., 1990 ; Li and Horowitz, 2000 ; Schroeck et al., 2001 ; Suthasun et al., 2004 ; Lee and Kim, 1997 ; Kim et al., 2001). In the sequel, the dual-stage can increase the minimum-time control performance in such a manner that the tracking error occurred in coarse stage following the minimum-time trajectory is effectively compensated by the high bandwidth motion of fine stage.

Since the dual-stage mechanism has actuation redundancy, it is naturally accompanied by the problem on how to coordinate the dual motions for a target point. Above all, the fine stage movement could be easily saturated owing to the small travel range. To avoid this problem, as is commonly the case, the coarse stage and fine one are separately operated. However, to best utilize the capability of the dual-stage mechanism, it is necessary to properly define the null-motion between the two stages. In this paper, we investigate the null-motion control which was not discussed so deeply in other dual-stage papers. By regulating the null-motion into the direction to minimize the relative distance between the two stages, the range saturation of the fine stage can be possibly prevented.

This paper is organized as follows. In Section 2, the robust minimum-time control (RMTC) is developed, where the minimum-time trajectory (MTT) for a 2nd order mass-damper system is derived and a novel robust perturbation compensator (RPC) is proposed. In Section 3, the RMTC is applied to the dual-stage positioning mechanism, where a dual-stage control architecture including the null-motion control loop is suggested. In Sections 4 and 5, the proposed control schemes are validated through simulation and experiment. Finally, concluding remarks are followed in Section 6.

2. Robust Minimum-Time Control

To achieve the minimum-time control performance in real applications where model uncertainty and process noise are involved, a practical consideration should appended to the optimal control solution : $u(t)=-\mathrm{sgn}(h(x))$. Differently from the conventional methods in (Franklin et al., 1990 ; Friedland, 1996 ; Newman and Souccar, 1991 ; Pao and Franklin, 1993 ; Kim et al., 1999) which modify the switching function near the target region, a kind of feedforward approach is suggested in this section. As shown in Fig. 1, the robust minimum-time control (RMTC) in this paper consists of the minimum-time trajectory generator (MMT) and the robust perturbation compensator (RPC) based tracking controller. After all, the switching function has been removed in the controller but the robust tracking controller follows the minimum-time trajectory for a target point. In conventional near time-optimal schemes, the width of non-switching region (Franklin et al., 1990 ; Pao and Franklin, 1993 ; Kim et al., 1999) around the target point or the boundary layer (Newman and Souccar, 1991) along the switching function are determined through the tuning process to avoid chattering, whereas the RMTC is fundamentally free of chattering problem by giving up the switching control.

In (Hara et al., 2000 ; Uchida and Semba, 2002), we can find reference following techniques related to the minimum-time control of hard disk drives. They provided efficient ways to find a reference trajectory which can suppress residual vibrations

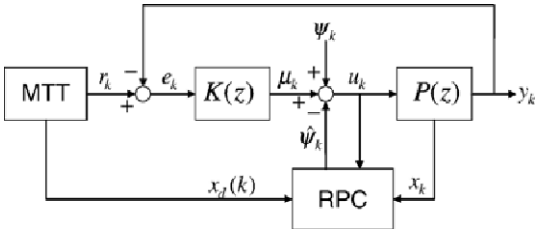

Fig. 1 Robust minimum-time control (RMTC) structure. MTT : minimum-time trajectory generator, RPC : robust perturbation compensator, $K(z)$: tracking controller, $P(z)$: plant

in track seek mode. However, it is too complex and time-consuming to get the best parameters and the solutions are based on simple double integrator model and moreover the solutions are quite different from real minimum-time trajectories. On the other hand, we stress that the friction term is needed to be included in developing the minimum-time trajectory and all system uncertainties which distort minimum-time performance should be effectively compensated by additional control function.

2.1 Minimum-time trajectory (MTT)

The minimum-time control problem is to find a solution which minimizes the cost function, $J=\int_{t_0}^{t_f} dt$ with the constraints of state equation, $\dot{x}=f(x,\tau,t)$ and the input limit $|\tau|\le\tau_{\max}$. As is well known, in terms of the Pontryagin's minimum principle, the minimum-time control law is given by the bang-bang control (Athans and Falb, 1966):

$$u(t)=-\mathrm{sgn}(h(x))=\begin{cases}-1 \text{ if } h(x)>0\\ +1 \text{ if } h(x)>0\end{cases} \quad (1)$$

where $h(x)$ is the so-called switching function and $u(t)$ is the normalized input (i.e., $u(t)\le 1$). In fact, the heart of minimum-time control problem is to determine the switching function. However, the solution was known for a few specific linear systems. For example, for a double integrator plant, $\ddot{y}=bu$, the switching function is given as $h(y,\dot{y})=y+(1/2b)\,\dot{y}\,|\dot{y}|$ for zero target condition, $\{y(t_f),\dot{y}(t_f)\}=\{0,0\}$.

Although a simple double integrator (or pure inertia) model was popularly used for the minimum-time control of many linear positioning mechanisms, it holds just for the applications where the frictional force is negligible. A good example is the track-seek mode in hard disk drives (Franklin et al., 1990 ; Pao and Franklin, 1993 ; Kim et al., 1999). However, for example, in positioning systems for semiconductor and flat panel display manufacturing equipments, the friction is a major obstacle to achieve fast and fine positioning. If the friction term is not considered in the minimum-time control of such applications, the control torques will have no margin to compensate

the frictional disturbances.

Hence, we consider the mass-damper system which includes viscous friction term as $H\ddot{y}+B\dot{y}=\tau$. This can be rewritten as $\ddot{y}+a\dot{y}=bu$ with $|u|\leq 1$ and also in state variable form, $\dot{x}_1=x_2$, $\dot{x}_2=-ax_2+bu$, with $x=[x_1\ x_2]^T=[y\ \dot{y}]^T$. Then, by integrating the 2nd order equation with the initial conditions: $y(t_0)=y_0$, $\dot{y}(t_0)=\dot{y}_0$, and $t=t_0$, we have

$$\dot{y}(t)=\frac{b}{a}+\left(\dot{y}_0-\frac{b}{a}\right)\exp\{-a(t-t_0)\} \tag{2}$$

$$y(t)=\left(\frac{1}{a}\dot{y}_0-\frac{b}{a^2}\right)(1-\exp\{-a(t-t_0)\}) +\frac{b}{a}(t-t_0)+y_0 \tag{3}$$

$$\rightarrow y(\dot{y})=\frac{b}{a^2}\ln\left(1-\frac{a}{b}|\dot{y}|\right)-\frac{1}{a}\dot{y}_0+y_0 \tag{4}$$

for the input $u=+1$ and

$$\dot{y}(t)=-\frac{b}{a}+\left(\dot{y}_0+\frac{b}{a}\right)\exp\{-a(t-t_0)\} \tag{5}$$

$$y(t)=\left(\frac{1}{a}\dot{y}_0+\frac{b}{a^2}\right)(1-\exp\{-a(t-t_0)\}) -\frac{b}{a}(t-t_0)+y_0 \tag{6}$$

$$\rightarrow y(\dot{y})=\frac{b}{a^2}\ln\left(1-\frac{a}{b}|\dot{y}|\right)-\frac{1}{a}\dot{y}_0+y_0 \tag{7}$$

for the input $u=-1$, respectively.

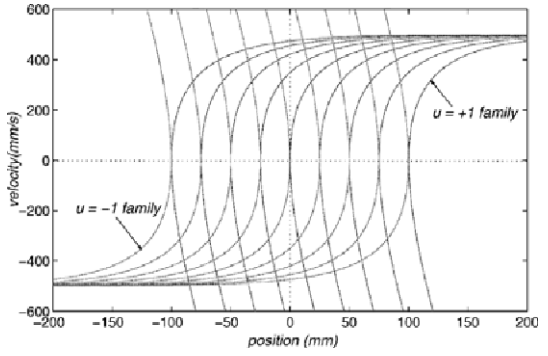

Fig. 2 Family of minimum-time trajectories for the plant, $\ddot{y}+10\dot{y}=5u$. The upper limit $\dot{y}=0.5$ m/sec of $u=+1$ curves and the lower limit $\dot{y}=-0.5$ m/sec of $u=-1$ curves are due to the frictional effect

The family of minimum-time trajectories for a specific plant is shown in Fig. 2, where the curves are not symmetric unlike double integrator plants because the viscous friction limits the velocity range to $|\dot{y}(t)|\leq b/a$. According to the above $u=+1$ and $u=-1$ family, the switching function for the target point, $x(t_f)=\{y(t_f),\ \dot{y}(t_f)\}=\{D,0\}$ is given by

$$h(x)=y-\mathrm{sgn}(\dot{y})\frac{b}{a^2}\ln\left(1+\frac{a}{b}|\dot{y}|\right) +\frac{1}{a}\dot{y}_0-D \tag{8}$$

and an example is denoted in Fig. 3.

Now, for the zero initial state: $\{y(t_0),\ \dot{y}(t_0),\ t_0\}=\{0,0,0\}$ and the target condition: $\{y(t_f),\ \dot{y}(t_f)\}=\{D,0\}$, it is straightforward to derive the following minimum-time trajectory (MTT) for a class of mass-damper systems, where the switching time (t_s) can be determined by equating the two trajectories for acceleration and deceleration phase.

(1) when $t\leq t_s$: acceleration phase ($u=+1$),

$$t_s=-\frac{1}{a}\ln(1-\sqrt{1-\exp\{-(a^2/b)D\}}) \tag{9}$$

$$y(t)=\frac{b}{a}t+\frac{b}{a^2}(\exp\{-at\}-1) \tag{10}$$

$$\dot{y}(t)=\frac{b}{a}(1-\exp\{-at\}) \tag{11}$$

$$y(\dot{y})=-\frac{b}{a^2}\ln\left(1-\frac{a}{b}|\dot{y}|\right)-\frac{1}{a}\dot{y}_0 \tag{12}$$

(2) when $t_s\leq t\leq t_f$: deceleration phase ($u=-1$),

$$t_f=t_s+\frac{1}{a}\ln\left(1+\frac{a}{b}\dot{y}(t_f)\right) \tag{13}$$

$$y(t)=y(t_s)-\frac{b}{a}(t-t_s) +\frac{1}{a}\left(y(t_s)+\frac{b}{a}\right)(1-\exp\{-a(t-t_s)\}) \tag{14}$$

$$\dot{y}(t)=\dot{y}(t_s)\exp\{-a(t-t_s)\} -\frac{b}{a}(1-\exp\{-a(t-t_s)\}) \tag{15}$$

$$y(\dot{y})=\frac{b}{a^2}\ln\left(1+\frac{a}{b}|\dot{y}|\right)-\frac{1}{a}\dot{y}_0+D \tag{16}$$

Figures 3 and 4 show the MTT for an arbitrary plant in comparison with the pure inertia case, where the asymmetry of velocity profile for the mass-damper system is caused by the fact that friction prevents acceleration but it is helpful in deceleration phase. As the moving range to the target gets longer, the asymmetry will become clearer.

Remark 1 : In deriving (9)-(16), we have used the mass-damper model $\ddot{y}+a\dot{y}=bu$ with viscous friction term only. However, if the Coulomb friction identification data are available, the equation of motion $\ddot{y}+a\dot{y}=b(u-f_c)$ with the normalized Coulomb friction $f_c>0$ can be readily utilized. In this case, the terms b in (2)-(4) and (9)-(12) are changed to $b(1-f_c)$ and the terms b in (5)-(7) and (13)-(16) to $b(1+f_c)$. Then, the MTT will be closer to that of actual systems.

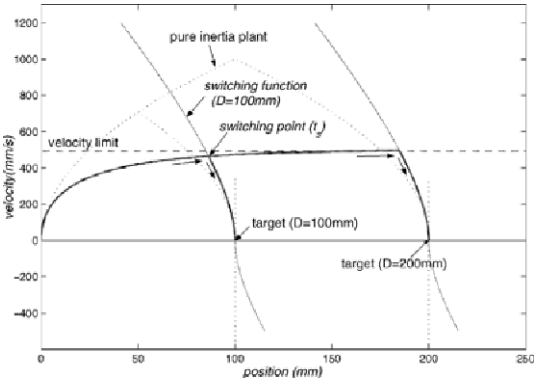

Fig. 3 Minimum-time trajectory (in phase plane) for the plant : $\ddot{y}+10\dot{y}=5u$ in comparison with the pure inertia plant : $\ddot{y}=5u$

2.2 Robust perturbation compensator (RPC)

The highlight to achieve the robust minimum-time control in Fig. 1 is the robust perturbation compensator (RPC) as well as the minimum-time trajectory in the former section. The performance of positioning system is degraded primarily by time-varying nonlinear friction caused by hard contact between moving parts as well as external disturbances. Therefore, the tracking control performance is greatly dependent upon how effectively the system uncertainty can be compensated. The disturbance observers (Kempf and Kobayashi, 1999 ; Komada et al., 2000) and time-delayed compensators (Youcef-Toumi and Reddy, 1992 ; Mittal and Menq, 1997) were widely applied as a robust control technique, which were considered as a class of perturbation observers in (Kwon and Chung, 2002). The perturbation observer is characterized by the adaptive control property which can estimate the time-varying perturbation with respect to the nominal plant. In this section, the robust perturbation compensator (RPC) is formulated as an extended version of the class of perturbation observers.

First, we consider a discrete state-space model :

$$x(k+1)=Ax(k)+Bu(k)+\psi(k) \qquad (17)$$

where the perturbation $\psi(k)$ includes all unmodeled dynamics and external disturbances and satisfies the matching condition to the control input. Then, the perturbation can be equivalently

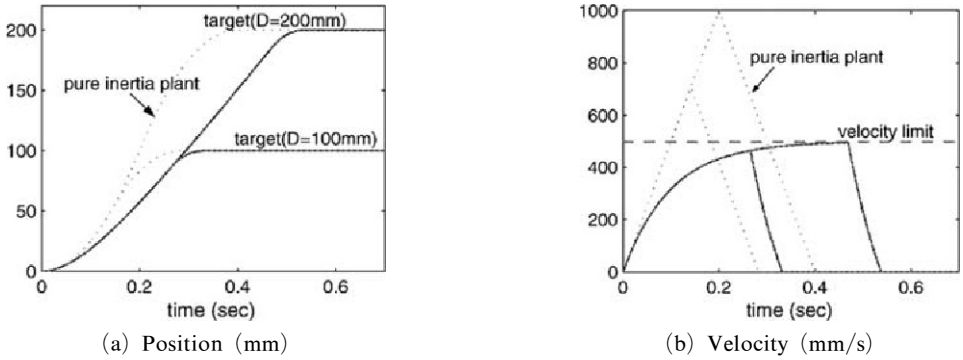

(a) Position (mm) (b) Velocity (mm/s)

Fig. 4 Minimum-time trajectory (position and velocity) for the plant : $\ddot{y}+10\dot{y}=5u$ in comparison with the pure inertia plant : $\ddot{y}=5u$ (when $D=100$ mm, $t_s=0.2657$ and $t_f=0.3315$)

descried as

$$\psi_{eq}(k) = B^{+}(x(k+1) - Ax(k)) - u(k) \quad (18)$$

Based on this indirect perturbation model, the following perturbation observer can be constructed.

$$\begin{aligned}\hat{\psi}_B(k) &= Q\psi_{eq}(k-1) \\ &= Q\cdot(B^{+}(x(k) - Ax(k-1)) - u(k-1))\end{aligned} \quad (19)$$

As shown, it consists of model parameters, control input, and state signals which are available at the current step k, where Q is the low pass filter to cut off high frequency harmonics. That is, the best estimate by the perturbation observer is the perturbation one-step before. Although the formulations are different, the notions of disturbance observers and time-delayed controllers are fundamentally correspondent to the above perturbation observer.

Here, if we replace the state signals $x(k)$ in (18) with reference signals $x_d(k)$, a feedforward type perturbation observer:

$$\hat{\psi}_F(k) = Q(B^{+}(x_d(k) - Ax_d(k-1)) - u(k-1)) \quad (20)$$

can be obtained as an alternative formulation to (19). It has the advantages of no requirement of feedback states by using reference signals. While the perturbation observer in (19) reconstructs the perturbation for the nominal plant, the feedforward perturbation observer in (20) can produce perturbation estimates with respect to the desired dynamics following the reference trajectory.

If we assume that the feedforward observer (20) is applied to the plant, the closed-loop error dynamics will be still perturbed by $\psi_R(k) = \psi(k) - \psi_F(k)$. Then, following the perturbation observer technique described above, the residual perturbation corresponding to the inter-sample variation can be further attenuated by $\hat{\psi}_R(k) = \psi_R(k-1) = Q\cdot\psi_{eq}(k-1) - \hat{\psi}_F(k)$. Finally, the total perturbation estimate at the current step is given by

$$\begin{aligned}\hat{\psi}(k) &= \hat{\psi}_F(k) + \hat{\psi}_R(k) \\ &= \hat{\psi}_B(k) + \hat{\psi} + \psi_F(k) - \hat{\psi}_F(k-1)\end{aligned} \quad (21)$$

which is referred to as the robust perturbation compensator (RPC) in this paper. It enables advanced perturbation compensation by utilizing both feedback signals and feedforward ones from the reference trajectory with no sensor noise and no dynamic lag.

In Fig. 1, the robust tracking control input is defined as the sum of the outputs from nominal feedback controller and RPC, i.e., $u(k) = \mu(k) - \hat{\psi}(k)$, where any control logic such as PD or PID rule can be chosen for the feedback controller. If the feedforward loop to the RPC is cut in (21), it is just equal to the standard perturbation observer in (19). There exist some guidelines on how to choose the low pass filter Q in (Komada et al., 2000; Kwon and Chung, 2002). Considering the stability of the perturbation observer (19), an useful analysis can be found in (Kwon and Chung, 2002) but the feedforward observer (20) does not produce any stability issue as far as the control input is bounded.

Remark 2: With only the feedback part in (19), the perturbation compensation input can be rewritten as $\hat{\psi}(k) = \hat{\psi}(k-1) + B^{+}(x(k) - Ax(k-1)) - \mu(k-1)$ without considering low-pass-filtering. This means that the perturbation compensator integrates the latter part which is changed according to plant behavior. In other words, the perturbation compensator has the integral and adaptive control property.

3. RMTC for Dual-Stage Mechanisms

In the former section, the robust minimum-time control (RMTC) which combines MTT and RPC has been investigated as an alternative to the switching control based sub-optimal methods. By removing the nonlinear switching function in controller, the RMTC does not produce chattering or transient phenomena due to controller change. In this section, the RMTC is extended to the dual-stage mechanisms, the usage of which is widely expanded to the applications where both ultra precision and wide scanning range are simultaneously required: for example, alignment stage (Lee and Kim, 1997), machine tool (Kim et al., 2001), and micromanipulation systems as well as longtime concern about macro/micro robot manipulators (Sharon et al., 1993; Khatib, 1995) and dual-stage hard disk drive (Yen et al., 1990;

Schroeck et al., 2001; Li and Horowitz, 2000; Suthasun et al., 2004).

3.1 Inertial property of dual-stage mechanism

In robot manipulators, the effective inertia, $\sigma_w(\Lambda)$ perceived at the end-effector along a specified direction w is given by $\sigma_w(\Lambda)=1/(w^T\Lambda^{-1}w)$, where $\Lambda(x)=(JA^{-1}J^T)^{-1}$ is the operational space kinetic energy matrix of a manipulator with A the manipulator inertia matrix and J the Jacobian between joint velocity and end-effector one (Khatib, 1995). Then, in macro/micro (or coarse/fine) manipulators, the effective inertia satisfies the following relationship.

$$\sigma_w(\Lambda_o)<\sigma_w(\Lambda_m) \tag{22}$$

in the direction of motion w, where Λ_o and Λ_m are the operational space kinetic energy matrices associated with the overall macro/micro manipulator and the single micro manipulator, respectively.

In the dual-stage model shown in Fig. 5 with the definitions of coordinates (y_1, y_2) and inertias (H_1, H_2), the dual-stage has the Jacobian $J=[1\ 1]^T$ and the inertia matrix $A=\mathrm{diag}\{H_1, H_2\}$ and the fine stage inertia is $\Lambda_m=H_2$. If we apply the above principle to the dual-stage mechanism, the effective inertia H_{eff} at the end-point of dual-stage along the task space coordinate y can be readily derived as

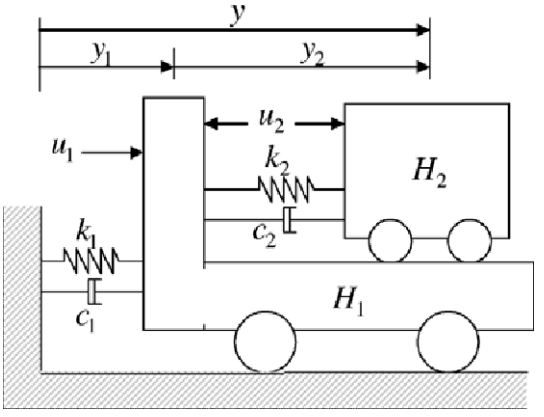

Fig. 5 Dual-stage model. (c_1, c_2) : viscous damping coefficients. (k_1, k_2): spring constants

$$H_{eff}=\frac{1}{[1\ 1](\mathrm{diag}\{H_1,H_2\})^{-1}[1\ 1]^T}=\frac{H_1H_2}{H_1+H_2}<H_2 \tag{23}$$

This means that the effective inertia perceived at the end-point gets smaller than independent stages and the dual-stage can produce larger accelerations.

3.2 Dual-stage control

The equations of motion for the dual-stage model in Fig. 5 can be described as

$$H_1\ddot{y}_1+c_1\dot{y}_1+k_1y_1=u_1+c_2\dot{y}_2+k_2y_2-u_2 \tag{24}$$

$$H_2\ddot{y}+c_2\dot{y}_2+k_2y_2=u_2 \tag{25}$$

which is a multi-input and multi-output (MIMO) system. If the cross couplings between the two stages are not negligible, it is natural to consider MIMO control design (Yen et al., 1990; Li and Horowitz, 2000). However, as is usually the case, when the stages are structurally very stiff for axial force and/or the coarse stage has much larger dimensions than the fine stage in parameter values, the motion of one stage almost does not affect the other one motion. In this case, the single-input and single-output (SISO) control design is acceptable (Suthasun et al., 2004; Lee and Kim, 1997; Kim et al., 2001) for the following decoupled model.

$$H_1\ddot{y}_1+c_1y_1=u_1+\psi_1 \tag{26}$$

$$H_2\ddot{y}_2+c_2=u_2+\psi_2 \tag{27}$$

where (ψ_1, ψ_2) are perturbations including nonlinear friction, external disturbance, and other model uncertainties which can be compensated by the RPC loop developed in the former section. Furthermore, the control architecture for dual-stage system can be changed depending on sensory condition, for example, whether the relative position between the two stages and the end-point sensing are available or not. Basically, the dual-stage servo should be designed so that the reference trajectory is tracked by the coarse stage with large power and long travel range while the fine stage corrects high frequency tracking errors.

In regard to the minimum-time control problem of the dual-stage, time-optimal seek trajec-

tories for dual-stage HDD were investigated in (McCormick and Horowitz, 1991 ; Yang and Pei, 1996), where the ideas were to make the coarse stage overshoot the target point as much as the fine stage stroke to reduce the seek time. In control point of view, such methods are not practical since they require the fine stage to be saturated. At the moment of range saturation, the fine stage will lose its capability of high bandwidth compensation motion.

By extending the RMTC in the former section to the dual-stage mechanism, the overall control architecture is denoted in Fig. 6, where the minimum-time trajectory (MTT) is generated for the coarse stage model and applied as a reference to both end-point and coarse stage. If the fine stage can successfully compensate the end-point tracking errors beyond the coarse stage bandwidth, the overall minimum-time control performance can be fairly enhanced by reducing the settling time. In Fig. 6, the end-point error is defined as $e=r-y$ and it is equal to $e=r-y=r-(y_1+y_2)=e_1-y_2$. This indicates that the end-point feedback to the fine stage in Fig. 6 can be altered by the relative position (y_2) feedback with the reference input of coarse stage error (e_1). In order to fully utilize fast and fine motion of fine actuator with small travel ranges, it is very important to maintain small tracking error in the coarse stage. The RPC added to the coarse actuator controller in Fig. 6 is expected to achieve the robust tracking performance in spite of perturbations such as nonlinear friction and abrupt disturbances. In the same way, the RPC for the fine stage could be added.

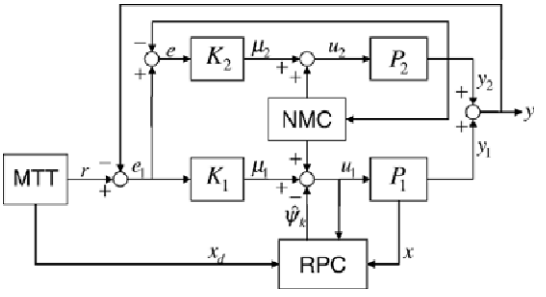

Fig. 6 Robust minimum-time control architecture for dual-stage mechanism. P_1 : coarse stage, P_2 : fine stage, NMC : null-motion controller

Since the movable range of most fine actuators is extremely small (usually, under hundreds of micron in piezoelectric actuators), the fine stage motion could be easily saturated to the travel limit for some large reference commands. During the saturation interval, the fine stage loses its capability of compensating high frequency disturbances and it may occur wind-up phenomena. Therefore, it is necessary to limit the input so that it does not over the movable range at current time. If the travel limit of fine stage is given by $|y_2|\leq R$, the movable range for the current position y_2 is equal to

$$S_{\min}=-(R+\mathrm{sgn}(y_2)|y_2|)<S(y_2)<R-\mathrm{sgn}(y_2)|y_2|=S_{\max} \tag{28}$$

Then, the input to the fine stage controller can be adjusted as

$$e^*=\begin{cases} S_{\max} & \text{if } e\geq S_{\max} \\ e & \text{if } S_{\min}<e<S_{\max} \\ S_{\min} & \text{if } e\leq S_{\min} \end{cases} \tag{29}$$

3.3 Null-motion control

In Fig. 6, when $e_1\rightarrow 0$ by the K_2 controller and $e\rightarrow 0$ by the K_2 controller, it results in $y_2\rightarrow 0$ naturally. However, the null-motion control (NMC) in this section is to accelerate the restoring action of $y_2\rightarrow 0$ using the internal motion of dual-stage. In a dual-stage mechanism, due to the extra degree of freedom, a null-motion exists between the two stages which do not produce end-point motions. By using the null-motion capability of the dual-stage, another set of control inputs can be determined to minimally keep the distance of the fine stage from the middle point without perturbing the end-point motion. However, this problem has not been considered in other dual-stage papers. As shown in Fig. 7, the null-motion control input (n_1, n_2) enables to coordinate the dual-stage motion into the direction of extending the movable range of fine stage for the same end-point positions.

In fact, the null-motion control is a well-established topic for robot manipulators with kinematic redundancy. In redundant mechanisms, the static force relationship between end-effector (F)

and joints (τ) takes the following form:

$$\tau = J^T F + (I - J^T J^{T+})\,\tau_o \tag{30}$$

where J is the Jacobian matrix and the second part corresponds to the null-space joint torques. In (30), J^{T+} is the generalized inverse of J^T and τ_o is an arbitrary generalized joint torque vector which will be projected onto the null space of J^T. By the way, a generalized inverse of J^T with which the null-space joint torques do not produce any operational acceleration at the end-point (i.e, which satisfies the so-called dynamic consistency) is given by the inertia weighted pseudo-inverse (Khatib, 1995):

$$\bar{J}(q) = A^{-1} J^T (J A^{-1} J^T)^{-1} \tag{31}$$

where A is the manipulator inertia matrix.

Hence, the null-motion control inputs which do not dynamically affect the task space (end-point) motion can be determined as

$$\tau_n = (I - J^T \bar{J}^T)\,\tau_o \tag{32}$$

When applying the above equation to the dual-stage model in Fig. 7 with $J = [1\ 1]$ and $A = \mathrm{diag}\{H_1, H_2\}$, the NMC input is readily derived as follows.

$$\tau_n = \begin{Bmatrix} n_1 \\ n_2 \end{Bmatrix} = \begin{bmatrix} -\frac{1}{4}\left(\frac{H_1+H_2}{H_2}\right) \\ 1-\frac{1}{4}\left(\frac{H_1+H_2}{H_2}\right) \end{bmatrix} \tau_o \tag{33}$$

For example, if the generalized joint torque is given by the following PD rule:

$$\tau_o = -k_P y_2 - k_D \dot{y}_2 \tag{34}$$

the input (33) will attract the fine stage to the middle point while not perturbing the end-point motion.

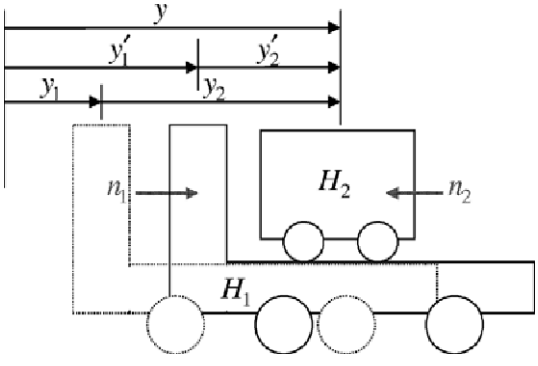

Fig. 7 Effect of null-motion control (NMC). (y_1, y_2): with no NMC, (y_1', y_2') : with NMC

4. Simulation Study

PTOS vs. RMTC

Now, it is verified how much the RMTC is beneficial than other sub-optimal methods through time-domain simulations. On behalf of sub-optimal methods, we select the PTOS (proximate time-optimal system) algorithm (Franklin et al, 1990). Although the original PTOS was developed for pure inertia plants, it can be modified for mass-damper systems as follows.

$$u(t) = -\mathrm{sat}\left(\frac{h^*(x)}{\Phi}\right) = \begin{cases} -\mathrm{sgn}(h^*(x)) & \text{if } |h(x)| > \Phi \\ -\dfrac{h^*}{\Phi} & \text{if } |h(x)| \le \Phi \end{cases} \tag{35}$$

where Φ is the boundary layer along the switching function $h(x)$ in (8) and the modified switching function $h^*(x)$ is given by

$$h^*(x) = \begin{cases} h_1(x) = -e(t) - \mathrm{sgn}(x_2)\dfrac{b}{a^2}\ln\left(1+\dfrac{a}{b}|x_2| - \Phi\right) \\ \qquad\qquad +\dfrac{1}{a}x_2 & \text{if } |e(t)| > y_l \\ h_2(x) = -e(t) + k_1 x_2 & \text{if } |e(t)| \le y_l \end{cases} \tag{36}$$

with $x_1 = y$, $x_2 = \dot{y}$, $e(t) = D - x_1(t)$ the position error, and y_l the width of linear region. Given the value of y_l, the other parameters Φ and k_1 can be determined using the continuity condition at $(x_1, x_2) = (y_l, v_l)$: $h_1(x) = h_2(x)$ and $h_1'(x) = h_2'(x)$.

While, the RMTC algorithm is the Fig. 1 itself. Given the model parameters (b, b), the MTT in (9)-(16) can be readily obtained. In the case of zero-order hold (ZOH) sampled-data system with sample time T, the discrete-time model in (17) has

$$A=\begin{bmatrix} 1 & \frac{1}{a}(1-e^{-aT}) \\ 0 & e^{-aT} \end{bmatrix} \text{ and}$$
$$B=\begin{bmatrix} \frac{b}{a}\left(T+\frac{1}{a}(e^{-aT}-1)\right) \\ \frac{b}{a}(\frac{b}{a}(1-e^{-aT}) \end{bmatrix} \quad (37)$$

for a mass-damper system $\ddot{y}+a\dot{y}=bu$, which leads to the determination of the RPC input $\hat{\psi}(k)$ in (21). Then, the robust tracking control input is given by

$$\begin{aligned} u(k) &= \mu(k)-\hat{\psi}(k) \\ &= K_P e(k)+K_D\dot{e}(k)-\hat{\psi}(k) \end{aligned} \quad (38)$$

The plant model for the controller design is given by $a=10$ with $a=10$ and $b=5$, the same as in Figs. 3 and 4, but the real plant is assumed to be $\ddot{y}_r+a_r\dot{y}_r=b_r(u-f_c+d)$ with model uncertainty $a_r=a(1+\Delta_a)$ and $b_r=b(1+\Delta_b)$, Coulomb friction f_c, and external disturbance d. Considering the sensor model, the position measure is given by $x_1(k)=y_r(k)+v(k)$ where the sensor noise is $v(k)\sim N(0,\sigma^2)$ with $\sigma=1$ μm and the velocity is determined by the filtered derivative:

$$x_2(k)=wx_2(k-1)+(1-w)(x_1(k)-x_1(k-1))/T \quad (39)$$

with $w=0.3$ and the sampling time $T=1$ msec. In the simulations, PTOS parameters for a best performance were tuned as $y_1=0.1$mm, $\Phi=0.5$ mm, and $k_1=0.052$ and RMTC parameters were $K_P=90^2$, $K_D=2\times0.85\times\sqrt{K_p}$, and the Q-filter for RPC: $Q(z)=0.15/1-0.85z^{-1}$. The marginal input over $u=\pm1$ was assumed to be $|u|\leq1.3$. Figures 8 and 9 are the results for PTOS and RMTC respectively with the following four cases.

Case 1: No uncertainty is involved.
Case 2: 10% model uncertainty is considered as $a_r=1.1a$ and $b_r=1.1b$.
Case 3: Coulomb friction is inserted as $f_c=+0.1$ [V] for $\dot{y}>0$ and $f_c=-0.1$ [V] for $\dot{y}<0$.
Case 4: External disturbance $d(t)=0.2\sin(40t)$ [V] is added.

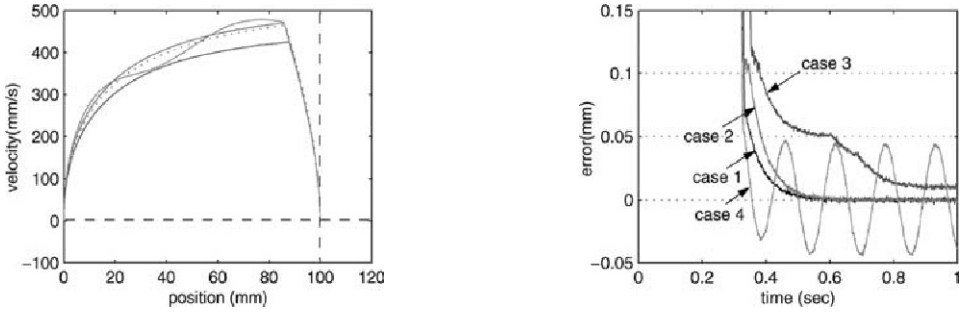

Fig. 8 Performance of PTOS with different perturbations (Case 1: no uncertainty, Case 2: parametric uncertainty, Case 3: Coulomb friction, Case 4: sinusoidal disturbance)

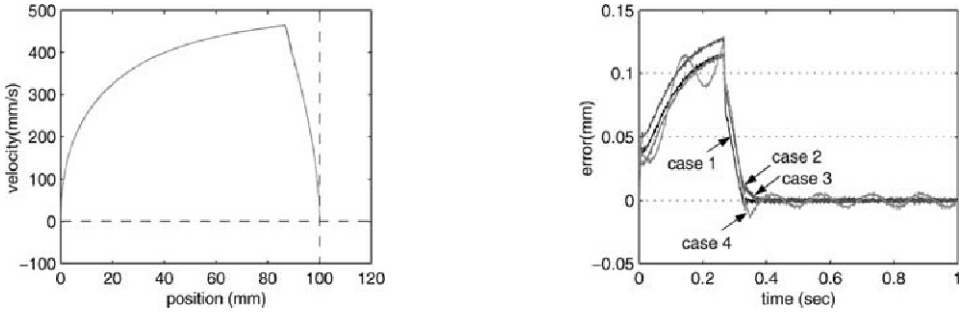

Fig. 9 Robust performance of RMTC with different perturbations (Case 1: no uncertainty, Case 2: parametric uncertainty, Case 3: Coulomb friction, Case 4: sinusoidal disturbance)

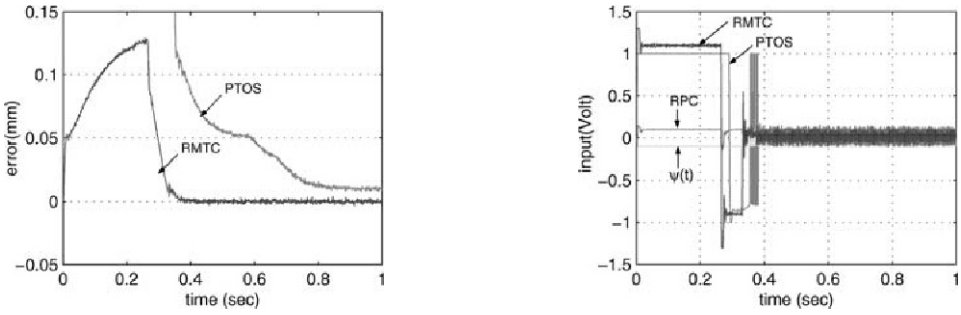

Fig. 10 Performance comparison between RMTC and PTOS (case 3 : Coulomb friction)

As shown, the PTOS performance is much dependent upon system uncertainty since it does not contain any function to compensate it, while the RMTC maintains relatively small settling time around the target ($D=100$ mm, $t_f=0.3315$) for all sort of perturbations. In Fig. 10 for Case 3, it shows that the RPC well reconstructs the Coulomb friction ($\psi(t)$). The robust performance of RMTC was enabled by the MTT following strategy from the initial time and the RPC to attenuate modeling error and other perturbations.

Dual-Stage RMTC

To confirm the utility of the RMTC for dual-stage mechanisms, we consider the coarse actuator model : $\dot{y}_1+a_1\dot{y}_1=b_1u_1$ with $(a_1, b_1)=(10,5)$ used in the above RMTC simulation and also assume the fine actuator model : $\dot{y}_2+a_2\dot{y}_2=b_2u_2$ with $(a_2, b_2)=(10,50)$. Then, the inertia and damping coefficient of the fine actuator correspond to the one tenth of the coarse actuator respectively, that is, $H_1=10H_2$ and $B_1=10B_2$ in (26) and (27). By applying the dual-stage RMTC loop in Fig. 6, the result in Fig. 11 was obtained for the same condition as the Case 3 in the above simulations. As shown, the coarse stage follows the minimum-time trajectory and the tracking error occurred in the coarse stage is well compensated by the high bandwidth motion of fine stage. As a result, the dual-stage maintains smaller tracking error at the end-point and the settling time to the target has been more reduced. In addition, comparing Fig. 11(a) with 11(b) explains the effect of the null-motion control (NMC). When the NMC input described in (33) was added to the both actuators, the relative motion between them was fairly reduced but the end-point motion was almost not changed. This is because the NMC makes the fine stage restore to its neutral position without perturbing the end-point motion.

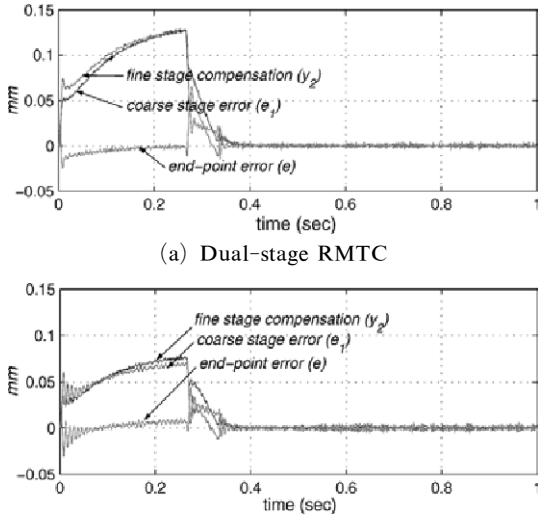

(a) Dual-stage RMTC

(b) Effect of NMC

Fig. 11 (a) Performance of the dual-stage RMTC (without null-motion control) (b) effect of null-motion control

5. Experiment

To experimentally validate the proposed robust minimum-time controller (RMTC), two linear stages were mounted in parallel as shown in Fig. 12, where both bottom and top stage are driven by BLDC electrical motors through ball-screw transmissions and the parameters for plant model : $H_i\ddot{y}+c_i\dot{y}_2=u-C_{f_i}(i=1,2)$ with $H_i[\mathrm{V}/(\mathrm{m/s^2})]$

the effective inertia, c_i[V/(m/s^2)] the viscous damping coefficient, and C_{f_i}[V] the Coulomb friction were identified as H_1=0.2020, c_1=2.25 \$ for the bottom stage and H_2=0.1665, C_2=1.35 for the top stage. As well, the Coulomb frictions were found as on the average C_{f_1}=0.11, C_{f_2}=0.09 in positive direction and C_{f_1}=0.13 and C_{f_2}= 0.29 in negative direction, respectively. Although the two actuators in Fig. 12 have the same mechanical and electrical characteristics, the coarse/fine dual-stage motion can be mimicked by adjusting the motor torque and control gain so that the top stage has much higher servo bandwidth (e.g., over five times) than the bottom stage.

First, it is investigated how much the robust perturbation compensator (RPC) can improve the tracking control performance comparing with the standard perturbation observer when a system is affected by arbitrary perturbation. We applied the control loop in Fig. 1 to the bottom stage in Fig. 12 but with the reference trajectory in Fig. 13(b) instead of MTT. The closed-loop setup consists of Pentium processor, D/A board, BLDC motor with encoder, and counter board. The result of Fig. 13(a) indicates the tracking error when the RPC in (21) and the standard perturbation observer in (19) are applied respectively. In both cases, the same nominal feedback control law: $\mu=k_P e+K_D\dot{e}$ and the same low pass filter: $Q(z)=0.1/1-09z^{-1}$ were used and the same sinusoidal disturbance input $\psi(t)=3\sin(20t)$ [V] was added to the control torques. As shown, the RPC enabled better tracking performance thanks to the residual perturbation compensation capability with both feedback and feedforward signals.

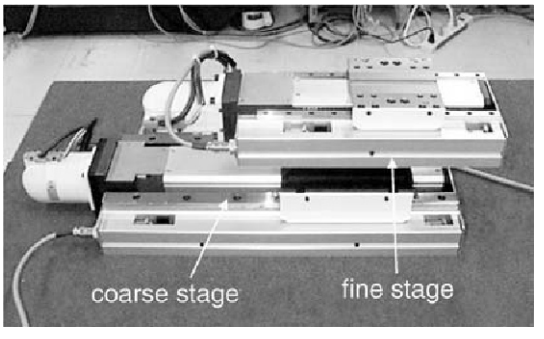

Fig. 12 Dual-stage experimental setup

Secondly, the RMTC loop for dual-stage in Fig. 6 was applied to the dual-stage setup in Fig. 12. The MTT in (9)-(16) was determined for coarse stage model parameters. Since the coarse stage and fine one in Fig. 12 actually have the

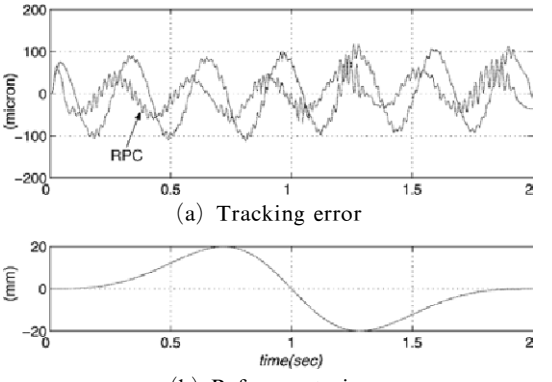

Fig. 13 (a) Performance comparison between the RPC (21) and the perturbation observer (19) for sinusoidal disturbance $\psi(t)=3\sin(20t)$ [V], (b) reference trajectory

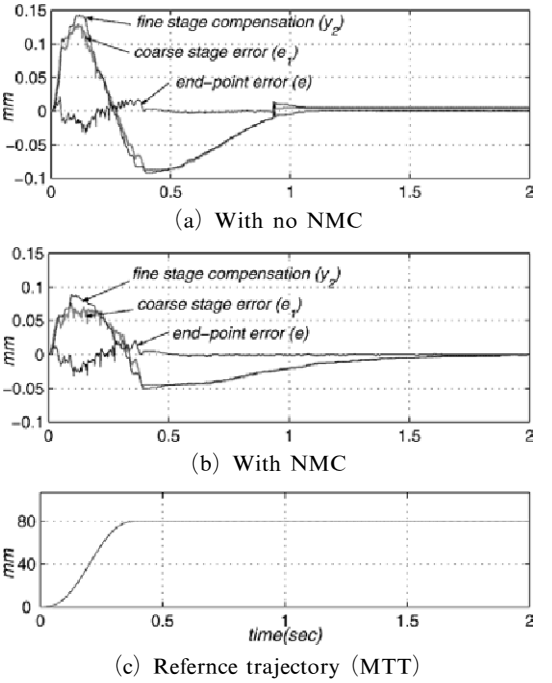

Fig. 14 Experiment of dual-stage RMTC: (a) without null-motion control. (b) with null-motion control. (c) reference trajectory

same physics, the same control law of PD control plus RPC was applied to both stages. But, in order to implement dual-stage motions by coarse actuator and fine one with different bandwidths, the control gains have been tuned so that the closed-loop bandwidth of fine stage is five times higher than that of coarse stage. As shown in Fig. 14, the tracking error occurred in the coarse stage was actively compensated by the fine stage motion and the end-point maintained small tracking error. As a result, the settling time of end-point to the target point has been fairly reduced by fast correction motion of fine stage.

As well, the relative motion between the two stages was much reduced by the null-motion control (NMC) action in Fig. 14(b) in comparison with the case of with no NMC in Fig. 14(a), but the end-point error was almost not changed. This validates that the NMC input (33) which satisfies the dynamic consistency attracts the fine stage to its neutral position but does not perturb the end-point (task space) motion. In the experiment, although no friction compensation scheme was applied, the coarse stage showed zero steady-state error. This is because the RPC loop works as a good friction compensator. Although the above experiment is a restrictive result where the real fine actuator is not involved, it is sufficient to prove the effectiveness of RMTC for dual-stage mechanism in Fig. 6.

6. Conclusion

In this paper, the robust minimum-time control (RMTC) was investigated as a reference following approach and it was extended to the coarse/fine dual-stage mechanism. It consists of the minimum-time trajectory (MTT) generator for a mass-damper system, the robust perturbation compensator (RPC) to mitigate system uncertainties, and the null-motion controller (NMC) for the dual-stage mechanism. It was stressed that the viscous friction term should be considered in generating minimum-time trajectories and the Coulomb friction should be compensated to achieve real minimum-time control. The simulation and experimental results suggest that the RMTC is a good alternative to other switching function based sub-optimal controllers, specifically when the system model is roughly identified and the positioning system is under heavy friction, abrupt load change, and large external disturbance.

References

Athans, M. and Falb, F. L., 1966, *Optimal Control*, McGraw-Hill.

Franklin, G. F., Powell, J. D., and Workman, M. L., 1990, *Digital Control of Dynamic Systems*, 2nd ed., Addison-Wesley.

Friedland, B., 1996, *Advanced Control System Design*, Prectice Hall.

Hara, S., Hara, T., Yi, L. and Tomizuka, M., 2000, "Novel Reference Signal Generation for Two-Degree-of-Freedom Controllers for Hard Disk Drives," *IEEE/ASME Trans. on Mechatronics*, Vol. 5, No. 1, pp. 73～78.

Kempf, C. J. and Kobayashi, S., 1999, "Disturbance Observer and Feedforward design for a High-Speed Direct-Drive Positioning Table," *IEEE Trans. on Control Systems Technology*, Vol. 7, No. 5, pp. 513～526.

Khatib, O., 1995, "Inertial Properties in Robotic Manipulation: An Object-level Framework," *International Journal of Robotics Research*, Vol. 13, No. 1, pp. 19～36.

Kim, B.-S., Li, J. and Tsao, T.-C., 2001, "Control of a Dual Stage Actuator System for Noncircular Cam Turning Process," *Proc. of the 2001 American Control Conference*, pp. 2549～2554.

Kim, B. K., Chung, W. K., Choi, H.-T., Lee, H. S. and Chang, Y. H., 1999, "Robust Time Optimal Controller Design for Hard Disk Drives," *IEEE Trans. on Magnetics*, Vol. 35, No. 5, pp. 3598～3600.

Komada, S., Machii, N. and Hori, T., 2000, "Control of Redundant Manipulators Considering Order of Disturbance Observer," *IEEE Trans. on Industrial Electronics*, Vol. 47, No. 2, pp. 413～420.

Kwon, S. J. and Chung, W. K., 2002, "Robust Performance of the Multiloop Perturbation Compensator," *IEEE/ASME Trans. on Mechatronics*, Vol. 7, No. 2, pp. 190～200.

Lee, C. W. and Kim, S. -W., 1997, "An Utraprecision stage for Alignment of Wafers in Advanced Microlithography," *Precision Engineering*, Vol. 21, pp. 113～122.

Li, Y. and Horowitz, R., 2000, "Track Following controller Design of MEMS Based Dual-Stage Servos in Magnetic Hard Disk Drives," *Proc. of the 2000 IEEE Int. Conference on Robotics and Automation*, pp. 953～958.

McCormick, J. and Horowitz, R., 1991, "Time Optimal Seek Trajectories for a Dual Stage Optical Disk Drive Actuator," *ASME Journal of Dynamic Systems, Measurement, and Control*, Vol. 113, pp. 534～536.

Mittal, S. and Menq, C. -H., 1997, "Precision Motion Control of a Magnetic Suspension Actuator Using a Robust Nonlinear Compensation Scheme," *IEEE/ASME Trans. on Mechatronics*, Vol. 2, No. 4, pp. 268～280.

Newman, W. S. and Souccar, K., 1991, "Robust, Near Time-Optimal Control of Nonlinear Second-Order Systems," *ASME Journal of Dynamic Systems, Measurement, and Control*, Vol. 113, pp. 363～370.

Pao, L. Y. and Franklin, G. F., 1993, "Proximate Time-Optimal Control of Third-Order Servomechanisms," *IEEE Trans. on Automatic Control*, Vol. 38, No. 4, pp. 560～580.

Schroeck, S. J., Messner, W. C. and McNab, R. J., 2001, "On Compensator Design for Linear Time-Invariant Dual-Input Single-Output Systems," *IEEE/ASME Trans. on Mechatronics*, Vol. 6, No. 1, pp. 50～57.

Sharon, A., Hogan, N. and Hardt, D. E., 1993, "The Macro/Micro Manipulator : An Improved Architecture for Robot Control," *Robotics and Computer Integrated Manufacturing*, Vol. 10, No. 3, pp. 209～222.

Suthasun, T., Mareels, I. and Al-Mamun, A., 2004, "System Identification and Controller Design for Dual Actuated Hard Disk Drives," *Control Engineering Practice*, Vol. 12, pp. 665～676.

Uchida, H. and Semba, T., 2002, "Reference Model Generation Using Time-Varying Feedback for Model-Following Control and Application to a Hard Disk Drive," *Proc. of the 2002 American Control Conference*, pp. 1389～1394.

Yang, J. -D. and Pei, X. -D., 1996, "Seek Time and Trajectories of Time Optimal Control for Dual Stage Optical Disk Drive Actuator," *IEEE Trans. on Magnetics*, Vol. 32, No. 5, pp. 3857～3859.

Yen, J. -Y., Hallamasek, K. and Horowitz, R., 1990, "Track Following controller Design for a Compound Disk Drive Actuator," *ASME Journal of Dynamic Systems, Measurement, and Control*, Vol. 112, pp. 391～402.

Yoshikawa, S., Harada, K. and Matsumoto, A., 1996, "Hybrid Position/Force Control of Flexible-Macro/Rigid-Micro Manipulator Systems," *IEEE Trans. on Robotics and Automation*, Vol. 12, No. 4, pp. 633～640.

Youcef-Toumi, K. and Reddy, S., 1992, "Analysis of Linear Time Invariant Systems With Time Delay," *ASME Journal of Dynamic Systems, Measurement, and Control*, Vol. 114, pp. 544～555.